# TTT-Cure Diagram of an Anhydride-Cured Epoxy System Including Gelation, Vitrification, Curing Kinetics Model, and Monitoring of the Glass Transition Temperature

**H. Teil,[1] S. A. Page,[2] V. Michaud,[1] J.-A. E. Månson[1]**

[1]*Laboratoire de Technologie des Composites et Polymères, Ecole Polytechnique Fédérale de Lausanne, Lausanne, Switzerland*
[2]*ABB Switzerland, Ltd., Corporate Research Baden-Dätwill, Switzerland*

Received 16 June 2003; accepted February 18, 2004
DOI 10.1002/app.20631
Published online in Wiley InterScience (www.interscience.wiley.com).

**ABSTRACT:** The curing reaction of an epoxy resin [diglycidyl ether of bisphenol A (DGEBA)] combined with a methyl-hexahydrophtalic anhydride (MHHPA) hardener and a benzyldimethylamine (BDMA) accelerator was studied over a temperature range of 60–140°C to build its isothermal time-temperature-transformation (TTT)–cure diagram. This includes gelation and vitrification measurements using rheological measurement techniques, monitoring of the glass transition temperature and the reaction kinetics by differential scanning calorimetry, and determination of the following critical glass transition temperatures: $T_{g0}$, $_{Gel}T_g$, and $T_{g\infty}$. A new curing kinetics model, based on the Sesták-Berggren model, was developed including both chemical- and diffusion-controlled stages of reaction. Then, the TTT-cure diagram was built by numerical integration of the kinetics model, and good agreement was obtained by comparison with experimental data. Additionally, for the first time, this model takes into account the incomplete cure, which occurs when the thermosetting system is cured below its ultimate glass transition temperature, leading to a more realistic description of the cure evolution after vitrification.
 J Appl Polym Sci 93: 1774–1787, 2004

**Key words:** curing of polymer; epoxy; gelation; glass transition; TTT-cure diagram

## INTRODUCTION

Epoxy systems are used in a large variety of application areas, among which coatings, electrical and electronic insulation, adhesives, composite materials, and construction are the major ones. They are known to provide great chemical and solvent resistances, mechanical responses ranging from great flexibility to high strength and hardness, good thermal and dimensional stabilities, and a high adhesive strength to most substrates, as well as very good electrical insulation properties.[1–3] However, the final performance of such materials is strongly dependent on the processing conditions applied. To fully appreciate the conversion of an epoxy system into a finished part, a full understanding of the curing process is required to determine the optimal curing conditions and thus reach the ultimate properties of the material. The isothermal time-temperature-transformation (TTT)–cure diagram, initially proposed by Gillham for thermosetting resins,[4–7] provides a useful framework for understanding the cure process of these materials. This diagram illustrates the various material state transitions that an epoxy system undergoes when cured under a given time-temperature scheme. Three main curves, namely, the gelation, vitrification / devitrification and full-cure curves, representing the major transitions undergone by the polymeric material, divide the diagram into several regions, each region corresponding to a distinct state of the thermosetting system, namely, liquid, sol glass, sol / gel rubber, sol / gel glass, gel rubber, and gel glass state.[7] Thus, a thermosetting TTT-cure diagram permits cure time-temperature paths to be chosen properly, so that the different material state transitions occur in a controlled manner and consequently give rise to predictable properties.

A complete characterization of an epoxy system is necessary to build its isothermal TTT-cure diagram. Its reaction kinetics must be measured and modeled over time and temperature. Curing kinetics of epoxy systems already have been studied extensively, giving rise to several curing kinetics models, especially with amine-cured epoxy systems[4,5,8,9] and, to a lower extent, with anhydride-cured epoxy systems.[10,11] Most of the models proposed so far depend only on the type of reaction involved (e.g., *n*th-order reaction or autocatalytic reaction). In addition, if the curing process is performed below the ultimate glass transition temperature of the system, the reaction kinetics decreases because diffusion processes become dominant at the

*Correspondence to:* J.-A. E. Månson (jan-anders.manson@epfl.ch).

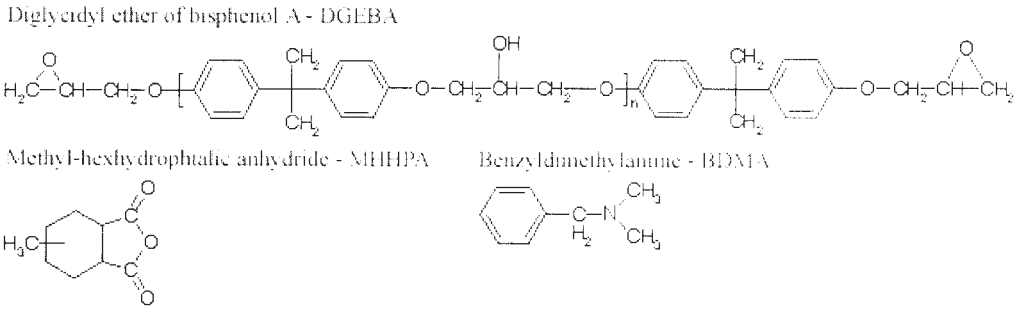


**Figure 1** Schematic chemical structures of the epoxy system components.

vitrification transition vicinity.[11] Consequently, to cover the entire course of the curing reaction, an overall reaction rate constant, which includes a diffusion-related component, usually is used to modify the kinetics models to take into account the diffusion-controlled stage of the reaction.[5,10] In parallel, gelation and vitrification times can be either experimentally evaluated using rheological measurement methods or determined by both the reaction kinetics and the consideration of the system component chemistry.[12,13] However, a careful choice of the measurement methodology must be performed so that kinetics and rheological values remain fully coherent. Then, by association of experimental data and a kinetics model, an isothermal TTT-cure diagram can be obtained using numerical integration.

In this article, a step-by-step methodology for the construction of the isothermal TTT-cure diagram of an anhydride-cured epoxy system is proposed. It includes evaluation of the curing reaction evolution over time, gelation and vitrification transition time measurements, and determination of the critical glass transition temperatures as well as the development of a new curing reaction kinetics model, which includes both the chemically and the diffusion-controlled stages of the cross-linking reaction and, for the first time, also takes into account incomplete conversion when operating below the ultimate glass transition temperature of the polymer.

## MATERIALS

The epoxy system under investigation comprises a diglycidyl ether of bisphenol A (DGEBA) resin (*Araldite CY 225*) combined with a methyl-hexahydrophthalic anhydride (MHHPA) curing agent (*HY 1102*) and a benzyldimethylamine (BDMA) accelerator (*DY 062*), all supplied by Vantico AG (Basel, Switzerland). The schematic chemical structures of the system components are represented in Figure 1. A stoichiometric resin-to-hardener mixing ratio is used, namely, 100 : 90 parts per weight, while one part per weight of accelerator is added. After mixing all the components, the system is degassed under vacuum. All of these operations are performed at room temperature.

## REACTION MECHANISMS

The curing reaction mechanisms of epoxy systems have been investigated extensively in the literature for a large variety of resin-hardener combinations.[1,2,14] Nowadays, uncatalyzed curing reaction mechanisms of epoxy resins with anhydride-based hardener are well understood.[15] In this particular case, anhydride groups react with hydroxyl groups to generate monoesters and carboxylic acid groups, the latter reacting then with epoxy groups to form diesters with new hydroxyl groups, which in turn react with other anhydride groups. When tertiary amines are used as accelerators, the curing reaction mechanisms are much more complex. In fact, the complexity of the mechanisms is linked mainly to the way the active sites are initiated. In the presence of a proton donor, the latter acts as a cocatalyst to form a complex with the amine, which then reacts with the anhydride group to form a carboxylate anion.[15,16] Then, the reaction mechanisms are similar to the ones involved in an uncatalyzed curing scheme. In the absence of a proton donor (e.g., pure monomeric epoxy without the hydroxyl group and pure anhydride group), the amine will react either with the anhydride group or with the epoxy group to initiate the reaction.[15] Indeed, the anhydride group will not react directly with the epoxy group and, consequently, it is necessary to first open a ring. The amine acts as a Lewis base accelerator and two main mechanisms have been proposed for this type of curing scheme.

The first type of reaction, which occurs between the tertiary amine and the anhydride group, is based on Fisher's work and often has been described in the literature.[1,2,14] In this case, the Lewis base accelerator reacts preferentially with an anhydride to generate a carboxylate anion. The latter reacts with an epoxy group to form a new anion and the anionic process continues until completion of the cure. The second type of reaction, which occurs

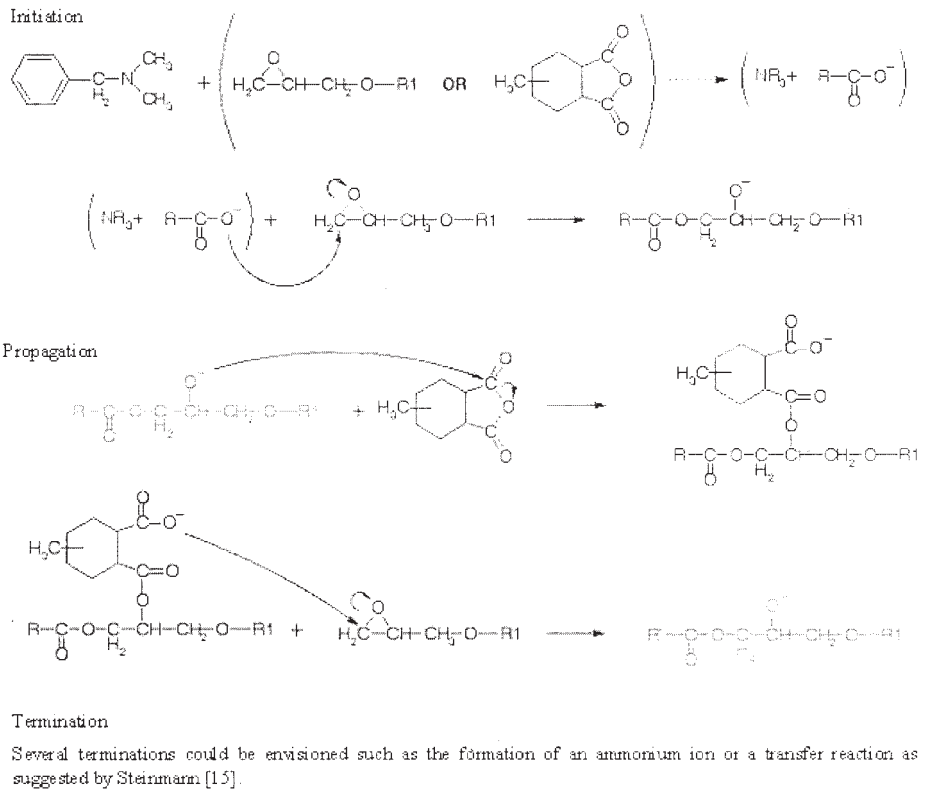


**Figure 2** Simplified reaction mechanisms scheme of an anhydride-cured epoxy system when tertiary amines are used as accelerators in the absence of a proton donor.

between the tertiary amine and the epoxy group, was proposed by Matejka et al.[16] using nuclear magnetic resonance (NMR) investigation. In this case, the tertiary amine reacts with the epoxy group to form an anion, which then reacts with an anhydride group to form a quaternary ammonium salt ($RN^{\oplus}$ $^{-}OOCR$). Finally, the $RCOO^{-}$ anion opens the epoxy ring, and a diester, together with a new anion, is simultaneously formed. This acidic curing reaction mechanism of a DGEBA resin catalyzed with tertiary amines hence is extremely complex and several side reactions can occur.[15] Note, however, that in an equimolar mixture the anhydride-based curing agent and the epoxy resin are consumed at the same rate and homopolymerization (i.e., etherification) almost never takes place.[16] In both types of curing reaction mechanisms proposed, the reaction of carboxylates with epoxy groups regenerates anions, which in turn reacts with other anhydride groups. A corresponding simplified reaction mechanisms scheme can be proposed as shown in Figure 2.

## CURING REACTION EVOLUTION

Calorimetric measurements were performed using a Perkin–Elmer differential scanning calorimeter (DSC) 7 (Perkin-Elmer, Norwalk, CT) calorimeter in a nitrogen atmosphere to determine the curing reaction evolution of the epoxy system under investigation. Ten- to 20-mg samples are encapsulated in aluminum DSC pans and then placed into the DSC cell at room temperature. The temperature is increased rapidly at $200°C \cdot min^{-1}$ up to the set curing temperature. Then, the heat flow is recorded until completion of the curing reaction. Figure 3 a shows the evolution of the heat flow over time for three different isothermal runs at 80, 100, and 120°C, respectively. Note that in several experiments, two exothermic peaks can be observed as shown in Figure 3 b. The inertia of heating can be considered as a first and simple explanation. Another possible cause can be the sample moisture content. Water is indeed a proton donor and, consequently, can act as a cocatalyst to form a complex with amines and subsequently react following the reaction mechanism described previously. This reaction is fast and exothermic and can correspond easily to the first peak sometimes observed.

After completion of the isothermal DSC measurements, the samples are scanned at $10°C \cdot min^{-1}$ up to 200°C to obtain the residual heat of the reaction. Then, the extent of the reaction or conversion $\alpha$ is calculated using

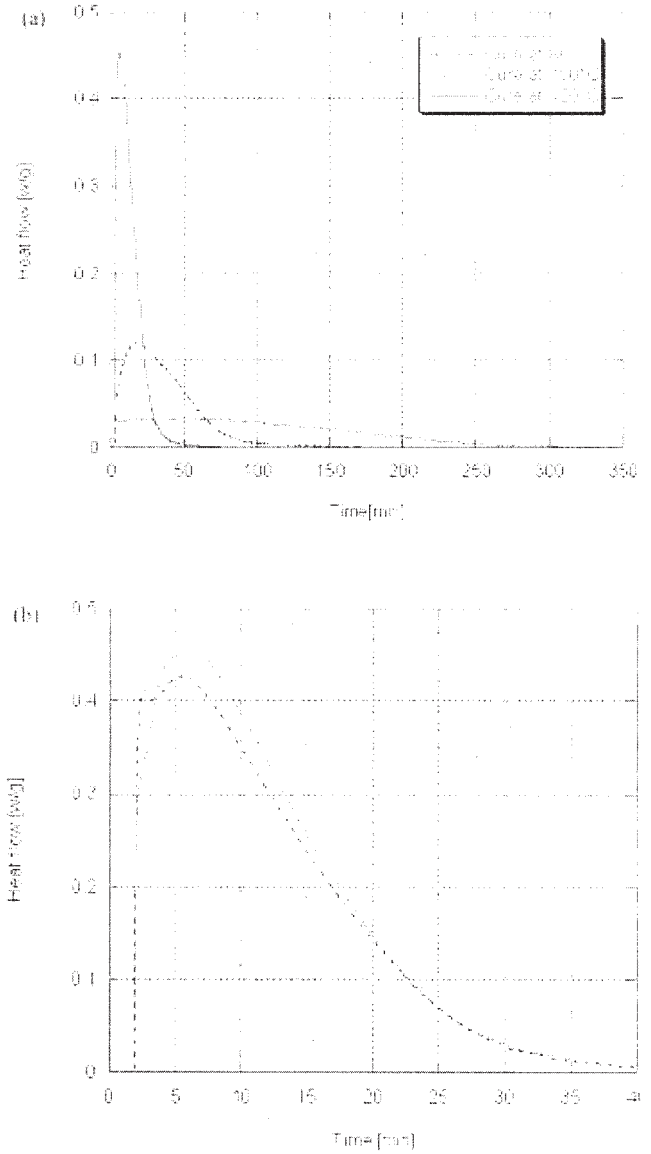


**Figure 3** (a) Isothermal DSC scans at 80, 100, and 120°C; (b) Isothermal DSC scans at 120°C with one showing two exothermic peaks.

$$\alpha(t) = \frac{\Delta H(t)}{\Delta H_{\text{total}}} \tag{1}$$

where $\Delta H(t)$ is the enthalpy of reaction at a given time $t$ and $\Delta H_{\text{total}}$ is the total enthalpy of reaction, i.e., the enthalpy of reaction obtained during the isothermal measurement added to the residual heat of reaction measured afterward. Figure 4 shows the extent of reaction over time at the three previously set temperatures, i.e., 80, 100, and 120°C. During the reaction process, the epoxy system evolves from a viscous liquid state to a glassy state leading to a three-dimensional molecular network. This material evolution is marked by two main and independent state transitions: gelation and vitrification.

## GELATION

Gelation corresponds to the irreversible liquid to sol / gel rubber transition and is characterized by the incipient formation of an infinite molecular network. At the molecular level, a critical number of intermolecular links has been exceeded[12] and one of the molecules has grown to reach the macroscopic scale.[17] Consequently, after gelation the epoxy system exhibits a viscoelastic behavior.[6] The gel point of an epoxy system is most commonly determined using rheological methods, even though other measurement methods such as solubility can be used also.[18] An infinite steady shear viscosity and a zero equilibrium modulus are the classical criteria used to define the gel point in rheology. However, such data are not directly accessible and extrapolation is required.[19] In practice, gelation is assumed to occur when the reduced viscosity $\eta_r$ [$\eta_r$ = viscosity ($\eta$) / initial viscosity ($\eta_0$)], reached $10^4$ [20] or when the steady shear viscosity reaches $10^3$ mPa · s and the material ceases to flow readily.[17] Gelation also can be detected by monitoring variations in the material dynamic mechanical properties. In a dynamic shear experiment, at a constant frequency, the gel point of an epoxy can be obtained as the intersection of the elastic modulus $G'(t)$ and the loss modulus $G''(t)$ curves,[19,21] i.e., when the loss tangent factor tan $\delta$ reaches the unity (ASTM standard D-4473). However, this method has been shown to be valid for stoichiometrically balanced systems only[22] or for those with an excess of hardener. Finally, the gel point is determined more commonly and precisely by the detection of tan $\delta$ independent of the measurement frequency.[22,23] In this investigation, the different gel points of the epoxy system under study are determined using the latter rheological method.

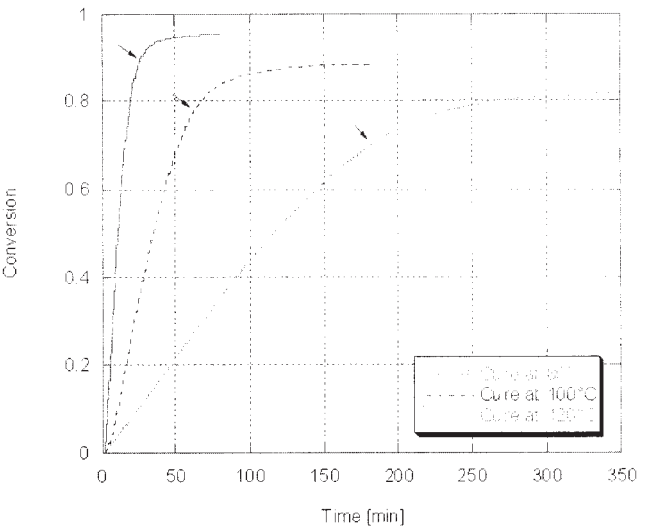


**Figure 4** Conversion or extent of reaction as a function of isothermal cure time at 80, 100, and 120°C.

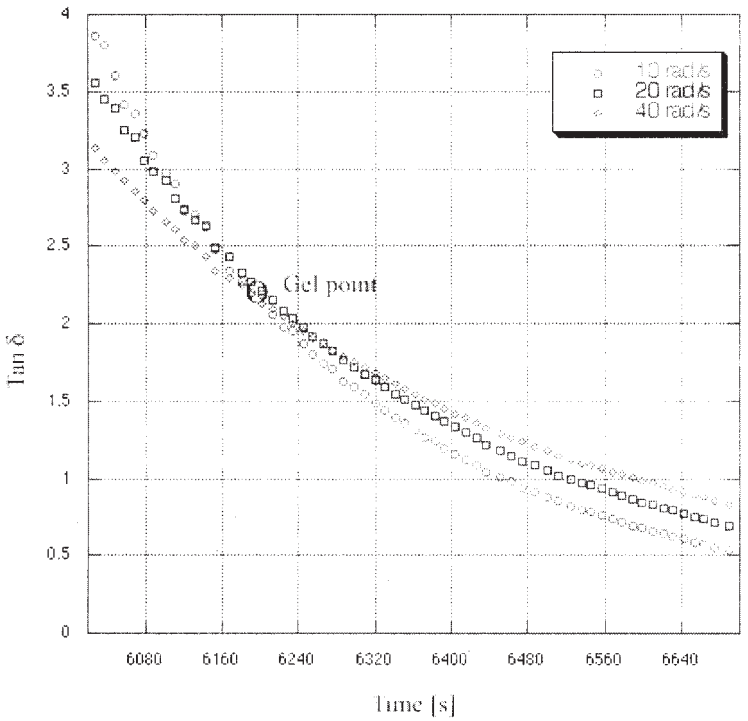


**Figure 5** Determination of the gel point as tan δ independent of the measurement frequency using a multiwave technique.

An Advanced Rheometric Expansion System rheometer (Rheometric Scientific, Piscataway, NJ) with 8-mm-diameter parallel plates is used. The resin samples are placed between the parallel plates 0.3 mm apart at room temperature and brought to the set cure temperature at a heating rate of 15°C · $min^{-1}$. The gel point is determined using a multiwave technique involving superposition and decomposition of the signal, which permits simultaneous collection of the data at several frequencies. The strain imposed is 100% and the gel point is determined from the intersection of the tan δ curves at frequencies of 10, 20, and 40 rad · $s^{-1}$, respectively, as shown in Figure 5. Note that the most critical parameter to be properly adjusted in this method is the applied strain, because approaching the gel point, the stress field applied to the material increases rapidly and may break the newly formed network. Table I summarizes the gelation time obtained at four different temperatures, i.e., 60, 80, 100, and 120°C. It is worth mentioning that by association of the extent of reaction with the gelation times obtained, it can be observed that gelation occurs at roughly 34% of conversion independently of the cure temperature imposed. The fact that the extent of reaction at gelation is independent of the cure temperature is a common observation[17,18] and similar results have been obtained already for a comparable epoxy system.[13] In other words, the conversion at the gel point can be considered as a constant for a given epoxy system [i.e., $\alpha\ (t_{gel},\ T) = \alpha_g$]. Consequently, a direct relationship between the gelation time $t_{gel}$ and the apparent curing kinetics constant $K_c$ can be established:[24]

**TABLE I**
**Gelation and Vitrification Times Measured Using Rheological Methods**

| Curing temperature (°C) | Gel time (min) | Vitrification time (min) |
|---|---|---|
| 60 | 349 | n.a. |
| 80 | 82 | 184 |
| 100 | 22 | 63 |
| 120 | 7 | 24 |
| 140 | NA | 19 |

$$t_{gel} = C' \times \left(\frac{1}{K_c}\right) \tag{2}$$

Assuming that the curing process is described by an overall activation energy $E_a$ and by application of an Arrhenius law such as $K_c(T) = C'' \times \exp(-E_a/RT)$, the following equation can be obtained:

$$\ln(t_{gel}) = C''' + \frac{E_a}{RT} \tag{3}$$

By plotting eq. (3), the overall activation energy can be obtained as shown in Figure 6. The $E_a$ value reached here is 71.1 kJ · $mol^{-1}$.

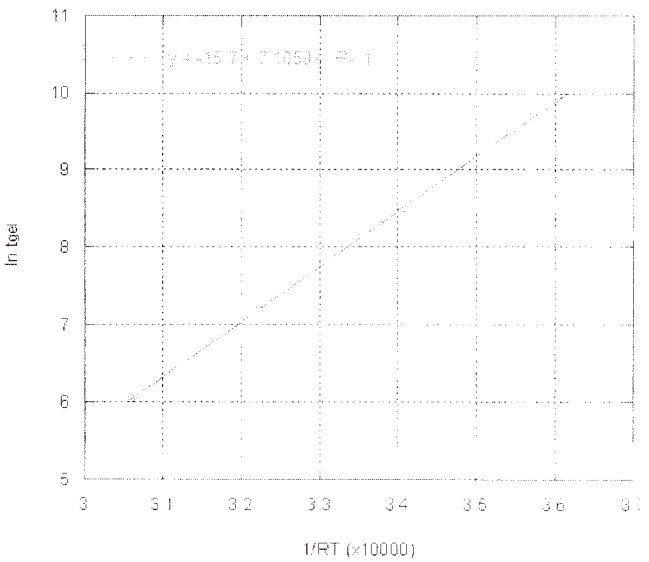


**Figure 6** Determination of overall activation energy by plotting eq. (3) ($E_{a1}$ = 71.1 kJ · mol$^{-1}$).

## VITRIFICATION

Vitrification corresponds to the irreversible liquid or sol / gel rubber to sol / gel glass transition and occurs when the glass transition temperature of the system reaches the isothermal curing temperature (i.e., $T_g = T_{\text{cure}}$).[6] This transformation induces a modification of the reaction kinetics by prohibiting further reactions, although a very slow diffusion-controlled reaction may occur in the glassy state.[25] As a result, the curing reaction kinetics goes from chemistry driven to diffusion controlled. No general criterion has been defined or accepted so far for the determination of the vitrification point and several methods based on different criteria are used arbitrarily. Consequently, a strong dependence of the measured values on the methodology used is observed. When using rheological methods such as a dynamic time sweep test, four criteria to determine the vitrification point are commonly accepted: the onset of the frequency dependence of $G'$, the peak of tan δ at 1 Hz, the peak of $G''$ at 1 Hz, or the end of the frequency dependence of $G'$.[23]

In this investigation, the vitrification point of the epoxy system under study is determined using the tan δ peak criterion obtained by a dynamic time sweep test with a strain of 0.1% and a frequency of 1 Hz, because this method provides the best agreement with the DSC results, as will be shown later. The same rheometer with 8-mm-diameter parallel plates, described in the previous section, is used. Resin samples are placed between the parallel plates 0.3 mm apart at room temperature and brought to the set cure temperature at a heating rate of 15°C · min$^{-1}$. The vitrification time obtained at four different temperatures, i.e., 80, 100, 120, and 140°C, are listed in Table I. The isothermal vitrification times are reported in Figure 4 (see arrows) and it can be clearly observed that as the extent of the reaction comes close to the vitrification point, its rate dramatically decreases. After vitrification, the conversion reaches a maximum value but never 100% for each set cure temperature.

## GLASS TRANSITION TEMPERATURES

Three critical temperatures are displayed on the TTT-cure diagram: the glass transition temperature of the uncured reactants (temperature below which the extent of reaction remains equal to zero) $T_{g0}$, the temperature at which gelation and vitrification occur simultaneously (and which therefore determine the upper limit temperature for storing reactive materials to avoid gelation[6]) $_{gel}T_g$, and the ultimate glass transition temperature of the thermosetting system $T_{g\infty}$. Temperatures $T_{g0}$ and $T_{g\infty}$ are measured directly using the same DSC equipment as previously described. Ten- to 20-mg samples are encapsulated in aluminum DSC pans, placed into the DSC cell at room temperature, and then scanned from −80 to 200°C at 10°C/min. Note that the samples are measured right after mixing in a liquid state for $T_{g0}$ determination and after a complete cure cycle including 1 week of postcuring at 160°C in a solid state for $T_{g\infty}$ determination. The respective values obtained are −40°C for $T_{g0}$ and 153°C for $T_{g\infty}$. Temperature $_{\text{gel}}T_g$ can not be obtained directly and will be deduced later according to the evolution of $T_g$ as a function of the conversion.

The determination of the evolution of the glass transition temperature as a function of the extent of reaction can be of great interest in the buildup of the TTT-cure diagram for an epoxy system. For this, several samples are cured in an oven and removed at different predetermined times. When moved out of the oven, the samples are immediately cooled down in liquid nitrogen and scanned in the DSC setup from −50 to 250°C at the heating rate of 10°C · min$^{-1}$. Fluctuations due to the opening of the oven are assumed negligible. Note, however, that for a short cure time, samples are cured directly into the DSC cell before being scanned in temperature. The epoxy system glass transition temperature is evaluated in this way at different times for two different isothermal cures, as shown in Figure 7. Similar to the results obtained with conversion, $T_g$ reaches a maximum value after vitrification but never its ultimate value for both set cure temperatures. Additionally, it is worth noting that when $T_g = T_{\text{cure}}$, the corresponding times agree well with the vitrification times measured using a rheological method (see Table I). Combining the results obtained in Figures 4 and 7, the evolution of $T_g$ as a function of $\alpha$ then can be obtained as shown in Figure 8. Assuming that one conversion is associated with one network structure and that one network

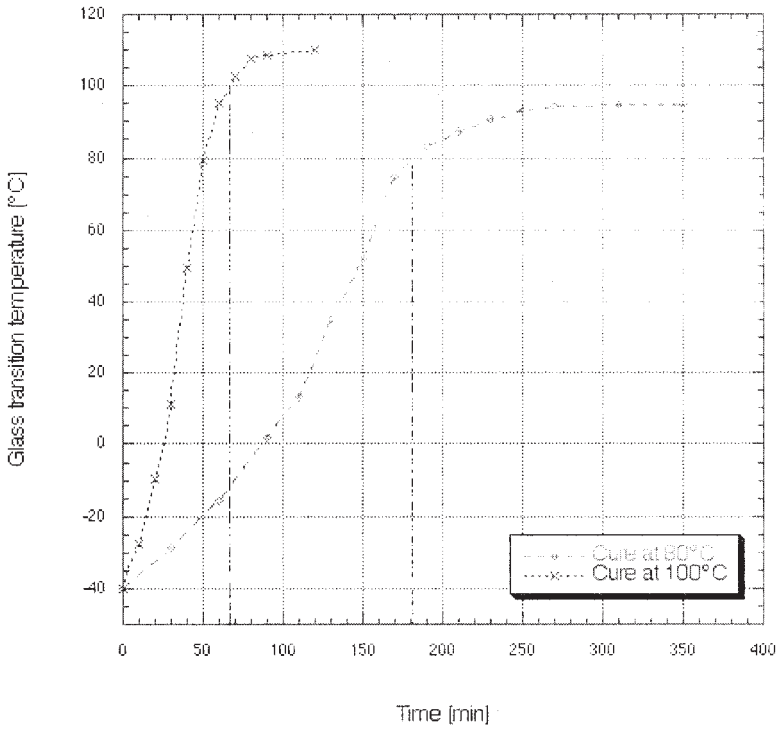


**Figure 7** Glass transition temperature as a function of isothermal cure time at 80 and 100°C.

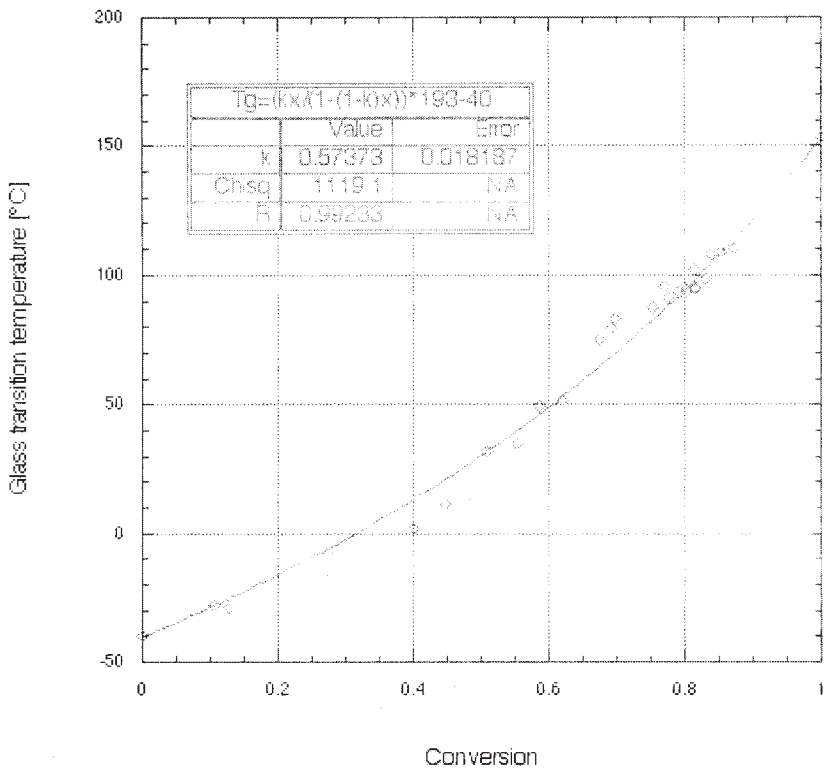


**Figure 8** Glass transition temperature as a function of conversion; a good correlation is obtained when fitting the experimental data obtained with eq. (4) (i.e., the DiBenedetto equation with $\lambda = 0.57$).

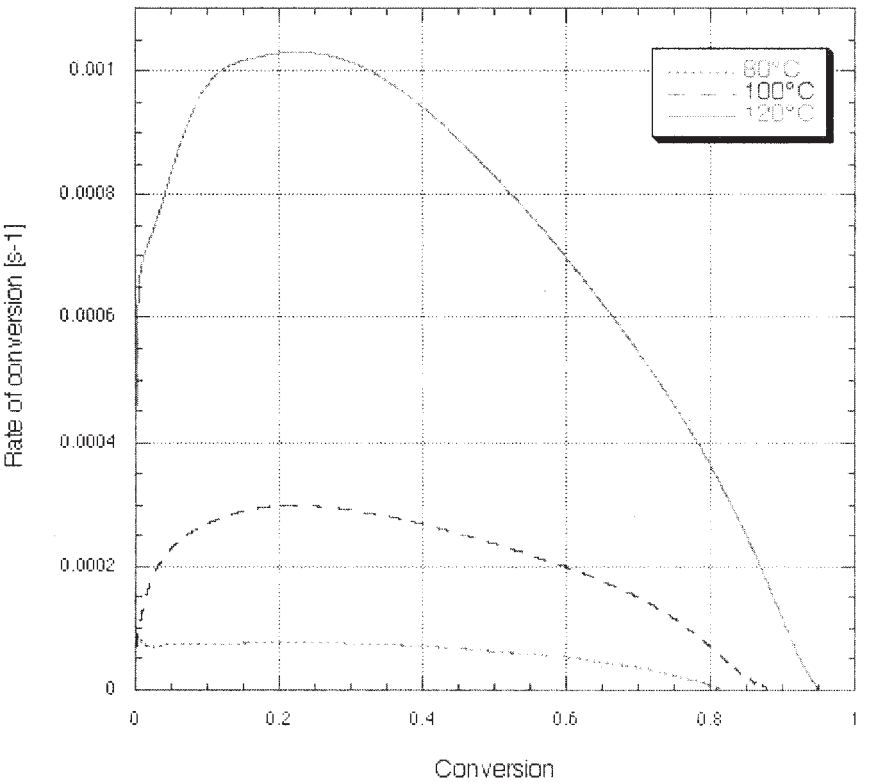


**Figure 9** Conversion rate as a function of conversion at 80, 100, and 120°C.

structure corresponds to one glass transition temperature; a direct relationship between $T_g$ and $\alpha$ can be foreseen. The most used constitutive equation for expressing $T_g$ as a function of $\alpha$ for a thermosetting system is the DiBenedetto equation[26] expressed as

$$\frac{T_g - T_{g0}}{T_{g\infty} - T_{g0}} = \frac{\lambda\alpha}{1 - (1 - \lambda)\alpha} \tag{4}$$

where λ is an adjustable parameter included between 0 and 1. When fitting eq. (4) to the results obtained here, as shown in Figure 8, a λ parameter of 0.57 is reached together with a good coefficient of correlation. Subsequently, for the present epoxy system, eq. (4) can be reformulated as

$$T_g = \frac{110.73\alpha}{1 - 0.43\alpha} - 40 \tag{5}$$

or

$$\alpha = \frac{T_g + 40}{0.43T_g + 127.78} \tag{6}$$

Equation (5) is very useful in determining the vitrification curve on the TTT-cure diagram. In the same way, ${}_{\text{gel}}T_g$ (at which gelation and vitrification occur simultaneously) can be determined using this relation. Vitrification occurs when the glass transition temperature reaches the cure temperature, hence, at the ${}_{\text{gel}}T_g$ point: $T_g = T_{\text{cure}} = {}_{\text{gel}}T_g$. In addition, it has been shown that the conversion at gelation is constant and roughly equal to 34%. Using eq. (5), ${}_{\text{gel}}T_g$ then can be evaluated and its value is here 4°C.

## CURING KINETICS MODELING

As previously introduced, during an isothermal cure below $T_{g\infty}$, the reaction process of an epoxy goes through two different stages. The first one is driven mostly by chemically induced reactions until $T_g$ of the system reaches $T_{\text{cure}}$, i.e., until vitrification. The thermosetting material then vitrifies and very slow diffusion-controlled reactions may occur during the second stage. Conversion of the polymer as well as its $T_g$ may increase again but at a much lower rate until the latter equals zero. Note, however, that the transition between these two stages does not occur suddenly, but rather needs a given period of time, which starts before vitrification. In this section, a complete curing reaction kinetics model, which would give a good description of the reaction evolution of the investigated epoxy system over time and temperature, will be defined.

As shown in Figure 9 for three different curing temperatures, i.e., 80, 100, and 120°C, the conversion

**TABLE II**
**Critical Conversion and Fitting Parameters Obtained When Using the Reaction Kinetics Model Expressed in Eq. (15)**

| Curing temperature (°C) | Critical conversion $\alpha_c$ (−) | Reaction rate constant $K_c$ (−) | Constant $C$ (−) | Parameter $m$ (−) | Parameter $n$ (–) |
|---|---|---|---|---|---|
| 80 | 0.74 | $0.1610^{-3}$ | 38.0 | 0.31 | 1.08 |
| 100 | 0.82 | $0.6210^{-3}$ | 38.1 | 0.33 | 1.12 |
| 120 | 0.89 | $2.2010^{-3}$ | 39.7 | 0.27 | 1.00 |

rate, $d\alpha / dt$, can be computed from the experimental DSC data obtained in Figure 3 a by using

$$\frac{d\alpha}{dt} = \frac{(dH/dt)}{\Delta H_{\text{total}}} = \frac{\phi}{\Delta H_{\text{total}}} \tag{7}$$

During the first stage driven by chemically induced reactions only, $d\alpha / dt$ can be described simply by a basic kinetics rate equation, such as

$$\frac{d\alpha}{dt} = K_c(T) \times f(\alpha) \tag{8}$$

where $f(\alpha)$ is a function of conversion and $K_c(T)$ is the apparent kinetics constant, which is a function of temperature only and generally is assumed to be of the Arrhenius form

$$K_c(T) = cst \times \exp\left( -\frac{E_a}{RT} \right) \tag{9}$$

The function $f(\alpha)$ is determined by the mechanisms and orders of reaction. Empirical models have been developed from best fittings of experimental data and improved by the introduction of additional parameters. The most well-known and most frequently applied model for epoxy reaction kinetics is the Kamal's autocatalytic model.[9,10,27] However, Montserrat and Málek[11] have indicated that the curing reaction kinetics of a DGEBA cured with both a hardener derived from a methyl tetrahydrophthalic anhydride and a tertiary amine as accelerator is described more accurately by the two-parameter autocatalytic model of Sesták-Berggren:

$$f(\alpha) = \alpha^m(1 - \alpha)^n \tag{10}$$

where $m$ and $n$ are two constants. When a thermosetting system is cured at a temperature higher than its ultimate glass transition temperature, diffusion phenomena may not affect the kinetics of reaction. However, in practice the cure of epoxy resins is performed at a temperature lower than $T_{g\infty}$ because of processing constraints. Different models have been proposed to describe the kinetics of thermosetting systems reaction during the diffusion-controlled stage by including a diffusion rate constant $K_d$. Most of them are based on the Williams-Landel-Ferry (WLF) equation.[10,28] For instance, Wisanrakkit and Gillham[4] have proposed a WLF-type equation, in which the absolute value in the denominator allows the application of the equation below the actual $T_g$ of the system

$$K_d = K_{\text{diff}} \exp\left[ \frac{C'(T - T_g)}{C'' + |T - T_g|} \right] \tag{11}$$

where $K_{\text{diff}}$ is a constant determined from experimental data. An alternative and interesting approach based on the reduction of the free volume during cure has been developed by Chern and Poehlein[8]:

$$K_d = K_c \exp[ - C(\alpha - \alpha_c)] \tag{12}$$

where $K_c$ is the chemically controlled rate constant, $C$ is a constant, and $\alpha_c$ is the critical conversion at which a three-dimensional cross-linked network is formed. Note that this latest definition corresponds to the conversion at gelation. However, the curing reaction becomes diffusion controlled as soon as the movement of the reactive functional groups is seriously restricted, i.e., in the vicinity of the vitrification point, as previously stated. The critical conversion $\alpha_c$ is subsequently reached at the vitrification point when $T_g$ reaches $T_{\text{cure}}$ and, consequently, can be calculated from eq. (6). The $\alpha_c$ values obtained at 80, 100, and 120°C are listed in Table II.

Finally, the overall reaction kinetics is a combination of chemically and diffusion-controlled reaction processes. At the beginning of the reaction process, the diffusion effects can be neglected, whereas in the vicinity of vitrification, the overall rate of reaction depends also on diffusion phenomena. Because the shift from a chemically to a diffusion-controlled reaction regime is progressive and does not occur exactly at a given time, an overall reaction rate constant $K_{\text{total}}$ has been proposed by Rabinowitch,[3,4,28] such as

$$\frac{1}{K_{\text{total}}} = \frac{1}{K_c} + \frac{1}{K_d} \tag{13}$$

As suggested by Boogh and Mezzenga,[29] by combining eqs. (12) and (13), the overall rate constant thus can be defined as

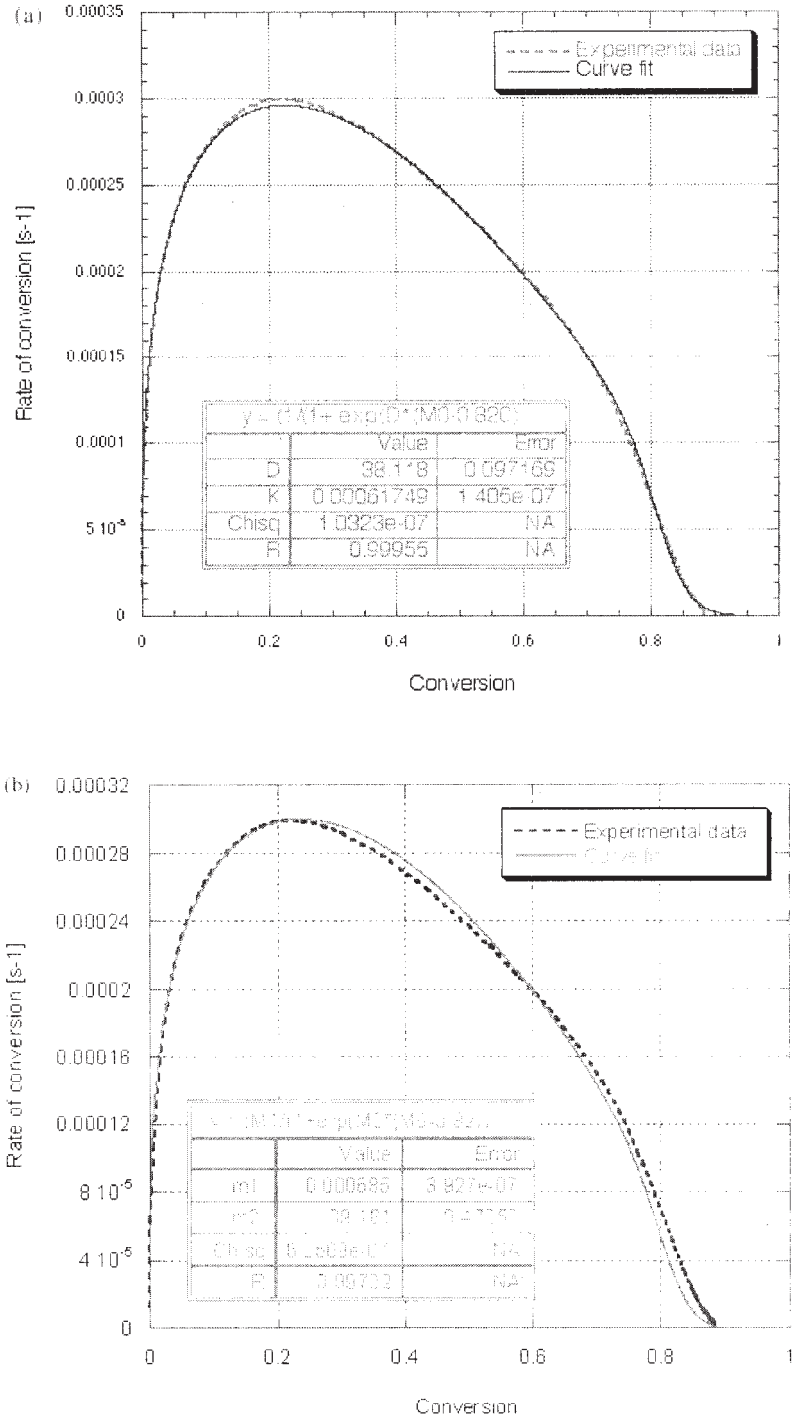


**Figure 10** Best fitting of the conversion rate at 100°C using (a) eq. (15) and (b) eq. (19). In the first case, the modeled reaction kinetics proceeds until full conversion of the polymer, and in the second case, the modeled reaction kinetics stops more realistically before full conversion.

$$K_{\text{total}}(T) = \frac{K_c(T)}{1 + \exp^{C(\alpha-\alpha_c)}} \tag{14}$$

$$\frac{d\alpha}{dt} = \frac{K_c(T)}{1 + \exp^{C(\alpha-\alpha_c)}} \alpha^m (1-\alpha)^n \tag{15}$$

Then, including eqs. (10) and (14) in eq. (8), the following overall reaction kinetics model can be obtained:

Figure 10 a shows a good fit of the conversion rate obtained at 100°C using eq. (15) and the fitting parameters $K_C$, $C$, $m$, and $n$ obtained at 80, 100, and 120°C are

**TABLE III**
**Critical and Ultimate Conversions and Fitting Parameters Obtained When Using the Reaction Kinetics Model Expressed in Eq. (19)**

| Curing temperature [°C] | Critical conversion $\alpha_c$ (−) | Ultimate conversion $\alpha_u$ (−) | Reaction rate constant $K_c$ (−) | Constant $C$ (−) | Parameter $m$ (−) | Parameter $n$ (−) |
|---|---|---|---|---|---|---|
| 80 | 0.74 | 0.83 | $0.1510^{-3}$ | 23.8 | 0.23 | 0.64 |
| 100 | 0.82 | 0.89 | $0.6910^{-3}$ | 39.2 | 0.32 | 0.87 |
| 120 | 0.89 | 0.96 | $1.9210^{-3}$ | 34.7 | 0.24 | 0.87 |

listed in Table II. Good correlations are obtained at each temperature. Note, here, that the overall activation energy $E_a$ also can be computed by plotting

$$-\ln K_c(T) = -\ln cst + \frac{E_a}{RT} \tag{16}$$

which is derived from eq. (9). The $E_a$ value obtained here is 74.8 kJ · mol$^{-1}$ and thus very similar to the value obtained previously by rheological measurements (i.e., 71.1 kJ · mol$^{-1}$). This kinetics model assumes that the epoxy will cure to complete conversion, whatever the curing temperature, as predicted by thermodynamics. However, when an epoxy system is cured below its ultimate glass transition temperature, the extent of the reaction will almost never reach the unity. During the cure process most of the reactive groups indeed are trapped or attached to the crosslinked network. Consequently, after vitrification, the molecular mobility is reduced markedly and the curing reaction will effectively cease before complete conversion of the polymer occurs.[8,28] Here, the modeled reaction kinetics continues, even if at a very low rate, after vitrification, until 100% of conversion at cure temperatures below $T_{g\infty}$, as shown in Figure 10 a.

Still based on the model of Sesták-Berggren, Sbirrazzuoli and Vyazovkin[30] have suggested an alternative form of the function of conversion $f(\alpha)$:

$$f'(\alpha) = \alpha^m(\alpha_u - \alpha)^n \tag{17}$$

where conversion $\alpha$ varies here between 0 and $\alpha_u$ and where $\alpha_u$ is the ultimate conversion obtained at a given cure temperature and can be expressed as

$$\alpha_u = \frac{\Delta H_{\text{end}}}{\Delta H_{\text{total}}} \tag{18}$$

where $\Delta H_{\text{end}}$ is the enthalpy at the end of the isothermal cure (i.e., after a long time, compared with usual cure schedules used for that system) and $\Delta H_{\text{total}}$ is the total enthalpy, i.e., the enthalpy of the isothermal cure added to the residual curing heat. Thus, eq. (15) can be rewritten as follows:

$$\frac{d\alpha}{dt} = \frac{K_c(T)}{1 + \exp^{C(\alpha-\alpha_c)}}\,\alpha^m(\alpha_u - \alpha)^n \tag{19}$$

A best fitting of the conversion rate obtained at 100°C using eq. (19) is shown in Figure 10 b and the fitting parameters $K_C$, $C$, $m$, and $n$ as well as the ultimate conversions $\alpha_u$, obtained at 80, 100, and 120°C, are listed in Table III. Very good and certainly more realistic correlations are obtained here at each curing temperature, because the modeled reaction kinetics ends up before complete conversion of the polymer is reached when the latter is cured below its $T_{g\infty}$. In addition, when computing again the apparent activation energy $E_a$ with the new $K_C$ values obtained here, 73.1 kJ · mol$^{-1}$ is reached, which is even closer to the value previously evaluated with rheological measurements (i.e., 71.1 kJ · mol$^{-1}$). Note that the drawback of this new reaction kinetics model is the need to evaluate experimentally the ultimate conversion at each curing temperature, because no model has been established yet to predict the ultimate conversion for a given cure temperature below $T_{g\infty}$.

## TTT-CURE DIAGRAM

Based on the curing kinetics models expressed in eqs. (15) and (19), the TTT-cure diagram of the epoxy system under investigation can now be built. Equation (15) is used to cover the entire range of time and temperature. For a given temperature of cure $T$, $K_c(T)$ is determined from eq. (16), $\alpha_c$ is calculated from eq. (6) with $T_g = T$, and then eq. (15) is numerically integrated to determine $\alpha$ as a function of $t$, i.e., $\alpha_T = f(t)$. This can be performed for an entire range of curing temperatures. Then, the isoconversion curves are obtained by joining all of the time-curing temperature points obtained for the same conversion $\alpha$. Two isocurves obtained in this manner (for $\alpha = 0.34$ and $\alpha = 0.60$) are presented in Figure 11 a. Here, the gelation curve corresponds to the 0.34 isoconversion curve. The three critical temperatures $T_{g0}$, $_{\text{Gel}}T_g$, and $T_{g\infty}$ also are displayed in Figure 11 a.

A one-to-one relationship [eq. (5)] between the glass transition temperature of the thermosetting system

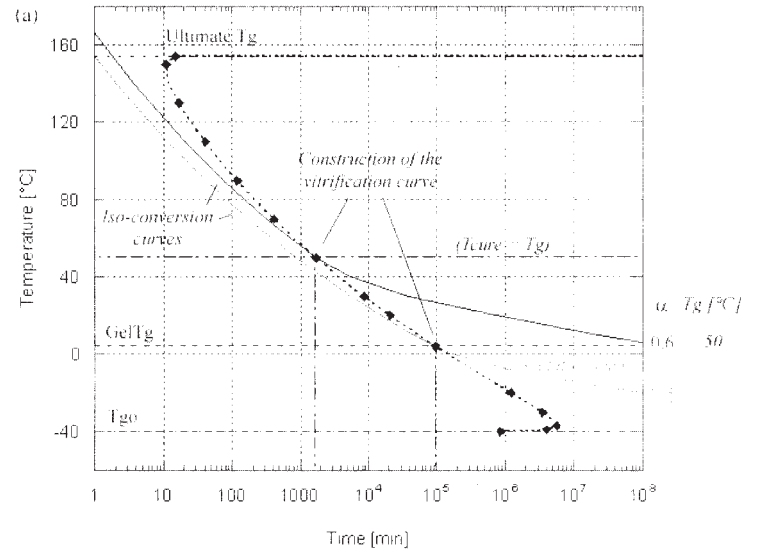
(a)
Ultimate Tg
Construction of the vitrification curve
Iso-conversion curves
(Tcure = Tg)
α Tg [°C]
0.6 50
Gel Tg
Tgo
Temperature [°C]
Time [min]

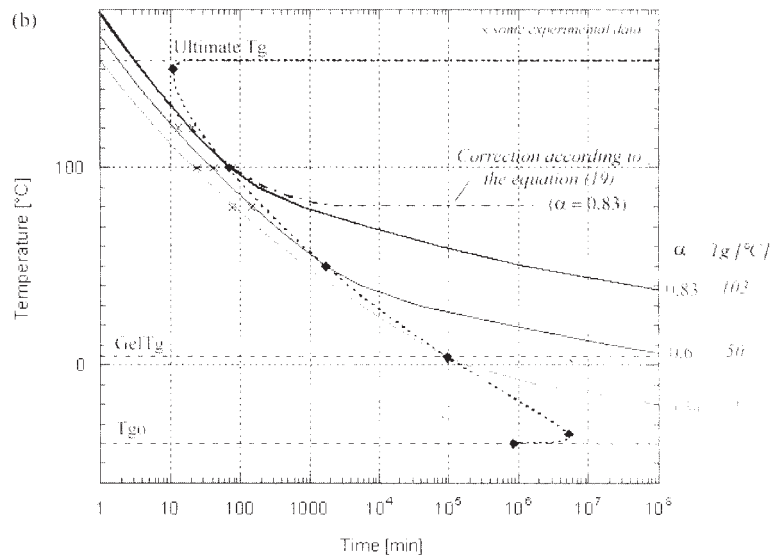
(b)
Ultimate Tg
Correction according to the equation (19)
(α = 0.83)
α Tg [°C]
0.83 10²
0.6 50
Gel Tg
Tgo
Temperature [°C]
Time [min]

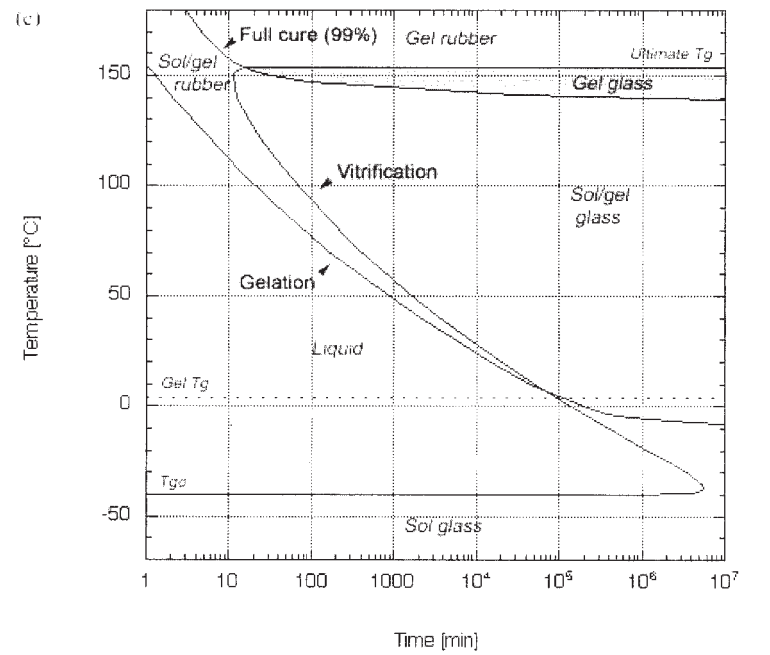
(c)
Full cure (99%)
Gel rubber
Ultimate Tg
Sol/gel rubber
Gel glass
Vitrification
Sol/gel glass
Gelation
Liquid
Gel Tg
Tgo
Sol glass
Temperature [°C]
Time [min]

under investigation and its extent of reaction $\alpha$ has been established as shown in Figure 8. Consequently, an iso-$T_g$ curve can be associated to each isoconversion curve. Then, the vitrification curve is determined using the intersection of the iso-$T_g$ curves and the $T_{cure} = T_g$ lines, which is the criterion of the vitrification point. Equation (19) then is used to take into account the incomplete cure in the sol / gel glass region and, hence, to correct the isoconversion curves, as shown in Figure 11 b. The former is numerically integrated similar to eq. (15), $\alpha_u$ being experimentally determined to obtain the same relationship as previously shown, i.e., $\alpha_T = f(t)$. A good agreement is obtained with experimental data. Additionally, the curve evolution after vitrification does look more realistic in the case of incomplete cure. However, the use of eq. (19) requires the experimental evaluation of the ultimate conversion $\alpha_u$ for each given curing temperature. The determination of a relationship such as $\alpha_u = f(T)$ would certainly allow obtaining a unique relationship that could display the entire isothermal TTT-cure diagram.

Finally, Figure 11 c displays a schematic and complete TTT-cure diagram of the epoxy system under investigation, respectively, displaying the isoconversion and iso-$T_g$ curves and the significance of each domain. The isothermal TTT-diagram is certainly a useful tool in the design of the cure cycle of thermosetting systems and, more specifically, in the optimization of their curing process. Note that although the diagram corresponds to an isothermal cure, it is still possible to envisage a variation of curing temperature assuming that no change in conversion occurs during a temperature ramp. In this case, it is possible to go from the curing temperature $T_1$ to the curing temperature $T_2$ by following the iso-$T_g$ or isoconversion curve from ($t_1$, $T_1$) to ($t_2$, $T_2$), $t_2$ becoming the new time of reference. This allows the optimization of multiple-steps cure or postcure cycles to ensure, e.g., that the glass transition temperature of the system remains higher than the actual temperature. Indeed, this could be useful for high-fiber-volume-fraction composite materials or large parts to avoid dimensional changes during postcuring.

## CONCLUSION

The acid curing reaction mechanisms of a DGEBA epoxy system catalyzed with a tertiary amine were investigated. As shown by the evolution of the rate of reaction and by the kinetic model based on the Sesták-Berggren equation, this reaction follows an autocatalytic model. However, this criterion is not verified directly by the propagation mechanism because only one anion is released at each step of the propagation stage. Consequently, we assume that the autocatalytic phenomenon results from the difference of kinetics between the initiation and propagation stages or other reaction mechanisms.

The kinetic study of this reaction showed that the cure progresses through two different stages. The first stage is chemically controlled until $T_g$ of the epoxy system reaches the curing temperature. The diffusion-controlled stage begins at the vicinity of the vitrification. An overall kinetic model based on the Sesták-Berggren equation is developed to describe the advancement of the reaction. Agreement between theoretical results and experimental data is good, but the model still does not take into account the incomplete cure when the cure process occurs below the ultimate glass transition temperature of the epoxy system. Then, a correction that incorporates the ultimate conversion reached at each curing temperature, taking into account the incomplete cure, was proposed. Thus, the isocurve evolution after vitrification is more realistic in the case of incomplete cure. Here, however, experimental data of the ultimate conversion reached at each curing temperature are needed. A direct relationship between the ultimate conversion and the temperature of cure would certainly allow obtaining a unique relationship that could display the entire isothermal TTT-cure diagram of a thermosetting system. Finally, critical temperatures such as $T_{g0}$, $_{Gel}T_g$, and $T_{g\infty}$ were evaluated and the complete isothermal TTT-cure diagram of the epoxy system under investigation was built.

This work was supported by ABB Switzerland, Ltd., Corporate Research.

**Figure 11** Buildup of the TTT-cure diagram from eqs. (15) and (19); (a) isocurves and vitrification curve built up; (b) correction for incomplete cure of the isocurves in the sol / gel glass region; (c) schematic but complete TTT-cure diagram of the investigated epoxy system.

## References

1. Penn, L. S.; Chiao, T. T. In Handbook of Composites; Lubin, G.; Van Nostrand Reinhold: New York, 1982; Chap. 5, p 57.
2. May, C. A.; Arroyo Research and Consulting Corporation. Composites; In Engineered Materials Handbook; ASM International: Metals Park, OH, 1987; Vol. 1, p 66.
3. Tai, H.-J.; Chou, H.-L. European Polym J 2000, 36, 2213.
4. Wisanrakkit, G.; and Gillham, J. K. J Appl Polym Sci 1990, 41, 2885.
5. Simon, S. L.; Gillham, J. K. J Appl Polym Sci 1992, 46, 1245.
6. Gillham, J. K. In Cure and Properties of Thermosetting Polymers; Kinloch, A. J., Ed.; Elsevier: Amsterdam, 1986; Chap. 1, pp 1–27.
7. Aronhime, M. T.; Gillham, J. K. Adv Polym Sci 1986, 78, 83.
8. Chern, C. S.; Poehlein, G. W. Polym Eng Sci 1987, 27, 788.
9. J. Y. Lee, H. K. Choi, M. J. Shim and S. W. Kim, Thermochimica Acta 2000, 343, 111.
10. Van Assche, G.; Swier, S.; Van Mele, B. Thermochim Acta 2002, 388, 327.
11. Montserrat, S.; Málek, J. Thermochim Acta 1993, 228, 47.

12. Flory, P. J. J Am Chem Soc 1941, 63, 3083–3097.
13. Khanna, U.; Chanda, M. Polymer 1996, 37, 2831.
14. Lee, H.; Neville, K. Handbook of Epoxy Resins; McGraw-Hill: New York, 1967; 800 pp.
15. B. Steinmann, J Appl Polym Sci 1989, 37, 1753.
16. Matejka, L.; Lövy, J.; Pokorny S.; Bouchal, K.; Dusek, K. J Polym Sci 1983, 21, 2873.
17. Hou, T. H.; Huang, J. Y. Z.; Hinkley, J. A. J Appl Polym Sci 1990, 41, 819.
18. Núñez, L.; Fraga F.; Castro, A.; Núñez, M. R.; Villanueava, M. Polymer 2001, 42, 3581.
19. Winter, H. H.; Chambon, F. J Rheol 1986, 30, 367.
20. Muzumdar, S. V.; Lee, L. J. Polym Eng Sci 1996, 36, 7.
21. In Standard Practice for Measuring the Cure Behavior of Thermosetting Resins Using Dynamic Mechanical Procedures, Designation D; ASTM Standard: Philadelphia, PA; pp. 4473–4490.
22. Chambon, F.; Winter, H. H. J Rheol 1987, 31, 683.
23. Lange, J.; Altmann, N.; Kelly, C. T.; Halley, P. J. Polymer 2000, 41, 5949.
24. J. M. Laza, C. A. Julian, E. Larrauri, M. Rodriguez and L. M. Leon, Polymer 1998, 40, 35.
25. Halley, P. J.; Mackay, M. E. Polym Eng Sci 1996, 36, 5.
26. Pascault, J. P.; Williams, R. J. J. J Polym Scit B Polym Phys 1990, 28, 85.
27. Flammersheim, H. J.; Opfermann, J. Thermochim Acta 1999, 337, 141.
28. Wise, C. W.; Cook, W. D.; Goodwin, A. A. Polymer 1997, 38, 3251.
29. Boogh, L.; Mezzenga R. In Comprehensive Composite Materials: 2.19 Processing Principles for Thermoset Composites; Kelly, A.; Zweben, C., Eds.; Elsevier: Amsterdam, 2000; Vol. 2, pp 671–769.
30. Sbirrazzuoli, N.; Vyazovkin, S. Thermochim Acta 2002, 388, 289.